Potential of a New Cone-Beam CT Software for Blooming Artifact Reduction

Carlos Estrela[1] , Marcus Vinicius C Costa[1] , Mike R Bueno[2,3] , Luiz Eduardo G Rabelo[1] , Daniel A Decurcio[1] , Júlio A Silva[1] , Cyntia R A Estrela[4,5]

[1]Department of Stomatology Sciences, UFG – Universidade Federal de Goiás, Goiânia, GO, Brazil
[2]Department of Radiology, SLMANDIC - Faculdade São Leopoldo Mandic, Instituto São Leopoldo Mandic, Campinas, SP, Brazil
[3]CROIF Oral Radiology Center, Cuiabá, MT, Brazil
[4]Department of Basic Sciences, School of Dentistry, UNIC - Universidade de Cuiabá, Cuiabá, MT, Brazil
[5]Department of Basic Sciences, School of Dentistry, UniEVANGÉLICA - Centro Universitário de Anápolis, Anápolis, GO, Brazil

Correspondence: Prof. Dr. Carlos Estrela, Praça Universitária s/n, Setor Universitário, 74605-220 Goiânia, GO, Brazil. Tel: +55-62-3209-6254. e-mail: estrela3@terra.com.br

This study evaluated the dimensions of intraradicular posts using a new cone beam CT (CBCT) software, and verified the potential of blooming artifact reduction. Sixty-three single-rooted human teeth were shaped, obturated, prepared for intracanal post placement and distributed into three groups: G1: anatomically customized prefabricated glass fiber posts; G2: low-fusion alloy posts; G3: gold alloy posts. After post fabrication and luting with RelyX U200®, specimens were sectioned axially at 9 mm from the root apex, and markings were made on the root surfaces (X-, Y- and Z-axes). The dimensions of the original posts (control group) were measured using a digital micrometer. CBCT scans of the teeth were obtained using a PreXion 3D Elite® scanner. Posts were measured on CBCT scans using DICOM files and the e-Vol DX software. A specific filter, Blooming Artefact Reduction (BAR), was developed to analyze intracanal posts. Statistical data were evaluated using the Van de Waerden nonparametric analysis of variance and, after that, normalized data were analyzed using the Tukey test. The level of significance was set at $\alpha = 5\%$. The measures of the anatomical prefabricated, low-fusion alloy and gold alloy intracanal posts obtained using the e-Vol DX CBCT software and a micrometer were not significantly different (p>0.05). The use of the BAR filter of the e-Vol DX software application did not induce any dimensional differences on CBCT scans of intracanal posts when compared with measurements made with a micrometer on original posts. The use of the BAR filter eliminated blooming artifacts.

Introduction

Recent scientific innovations have led to better tooth survival rates and greater predictability of root canal treatment prognosis (1,2). The incorporation of cone beam CT (CBCT) to procedures in endodontic clinical application have brought precision to diagnosis and planning, as well as greater safety for clinical decision-making and increased positive expectations of therapeutic success (3-5).

Dental solid and metal structures, composed of high-density materials, are responsible for artifacts that affect image contrast and become a confounding factor that changes quality and reduces the precision of the analysis of CBCT scans. Artifacts are any systematic discrepancy between the grayscale values of the reconstructed image and the actual attenuation coefficients of the original object (6). CBCT image artifacts may be responsible for several errors in image interpretation and, consequently, in clinical diagnosis (7). CBCT scans of teeth with obturation materials or intracanal posts show ghost images on areas around them, which mask the actual structure of the root canal or change the volume of the image of a high-density post (8-11). White contrast artifacts, known as blooming artifacts, increase the risk of clinical diagnostic

errors and have a direct impact on misinterpretations of imaging studies, which may have disastrous consequences for an endodontic treatment and lead, for example, to loss of a tooth.

Some strategies have been used to reduce or eliminate the effects of metal artifacts during CBCT image acquisition, postprocessing, reconstruction and other procedures (7,12-16).

A recent CBCT software package (e-Vol DX) (13) has been developed to reduce the occurrence of contrast artifacts produced by high-density materials, such as metal intracanal posts. As few studies have used this new software, the present study evaluated the dimensions of intraradicular posts using a new CBCT software and a digital micrometer, and verified the potential of blooming artifact reduction on CBCT scans.

Material and Methods

Tooth Preparation

Sixty-three human single-rooted teeth extracted for different reasons were selected and stored in 0.1% thymol until used. This study was approved by the Institutional Ethics Committee (approval under #06486919.0.0000.5083).

The teeth were removed from storage in thymol solution and immersed in 5% sodium hypochlorite for 30 min to remove external organic tissues. For sample selection, periapical radiographs were obtained to confirm that the pulp cavity was intact and that roots were fully formed, as well as to rule out calcifications, internal and external resorption, changes in dental development and previous endodontic treatment.

Standard access was prepared using #1013 round diamond burs (KG Sorensen, Cotia, SP, Brazil). Working length, set at 1 mm short of the apex, was determined and confirmed by visualization of the tip of a K-Flex #15 file (Dentsply/Maillefer, Ballaigues, Switzerland) at the apical foramen, which was then pulled back 1 mm. After cervical preparation, the teeth were cleaned and shaped using BioRace® instruments (FKG Dentaire, La Chaux-de-Fonds, Switzerland) to a final apical diameter corresponding to BR7 #60/0.02. The root canals were irrigated after each file change with 3 mL of freshly prepared 2.5% sodium hypochlorite solution. After that, root canals were dried and filled with 17% EDTA (pH 7.2) for 3 min to remove the smear layer. Root canals were again irrigated with 3 mL of 2.5% sodium hypochlorite solution and dried with absorbent paper cones. Finally, all teeth were obturated using gutta-percha and AH Plus™ (Dentsply/Maillefer, Ballaigues, Switzerland) using lateral condensation.

Standard root length was 13 mm. The coronal portion was removed using a 4" x 0.12" x 0.12" diamond wafering blade (Extec, Enfield, CT, USA) and an Isomet 1000 precision cutter (Buehler Ltd., Lake Bluff, IL, USA) under water spray and at a calibrated cutting speed of 250 rpm. Length was determined from the root apex using a 0.01-mm calibrated digital caliper (IV Electronic Caliper, Fowler/Sylvac, Crissier, Switzerland).

Specimens were randomly distributed into three groups: G1: anatomically customized prefabricated glass fiber posts (Exacto®, Angelus, Londrina, PR, Brazil) (n=21); G2: low-fusion alloy posts (Golden Cast®, Talmax, Curitiba, PR, Brazil) (n=21); G3: gold alloy posts (La Croix Au-Pd [LAU]®, La Croix Ligas Dentais Ltda, Rio de Janeiro, RJ, Brazil) (n=21).

The preparation of the root canals for the intracanal post included the removal of the obturating material using #3 Gates-Glidden and #1 Largo burs (Dentsply/Maillefer). The space for the intracanal post measured 8 mm, and 4 mm of obturating material was left in the apical third.

A #5 Exacto® post (Angelus) was used to manufacture the anatomically customized glass fiber posts. Anatomical customization consisted of checking the fit of the post in the prepared space, followed by immersion of the post in 24% H2O2 for 1 minute, rinsing, drying and applying silane (Angelus) to the whole surface for 1 minute. After preparation, the canal was isolated using a water-soluble gel (K-Y Gel®, Johnson's & Johnson's, São Paulo, SP, Brazil). A bulk fill composite resin (3M™ Filtek™ One Bulk Fill Restorative, Oral Care Solutions Division, Sumaré, SP, Brazil) was added incrementally to the post, according to the manufacturer's recommendations. After that, the set was introduced into the root canal and light cured for 5 min using a LED Radii-Cal® unit (SDI, Bayswater, Australia) at 1200 mW/cm², while at the stage of anatomical customization, and out of the prepared canal during the final 60 s. After anatomical customization of the glass fiber post, the canal was rinsed with distilled water and dried with absorbent paper points. Silane was applied to the anatomically customized glass fiber post, the post was cemented using a self-adhesive resin cement (RelyX U200®, 3M ESPE, Seefeld, Germany), and excess was removed using a #5 probe. Each surface was then light-cured for 60 s using a light-curing unit (LED Radii-Cal®, SDI, Bayswater, Australia) at 1200 mW/cm². The pattern for the metal intracanal posts was made using prefabricated posts (Pinjet®, Angelus) and a direct technique that uses a self-curing acrylic resin (Pattern Resin LS® Gc America Inc., Alsip, IL, USA). After that, the pattern was sent to a prosthetic laboratory to be cast in a low-fusion alloy (Golden Cast®, Talmax, Curitiba, SP, Brazil) for the specimens in Group 2, and in a gold alloy (La Croix Au-Pd - LAU®, La Croix Ligas Dentais Ltda, Rio de Janeiro, RJ, Brazil) for Group 3.

After the posts were cast, the previously prepared canals were rinsed with abundant distilled water and dried with absorbent paper points, and the posts were cemented as described above.

Measurement of Specimens Using a Micrometer

The 63 samples were sectioned axially using a 4" x 0.12" x 0.12" diamond wafering blade (Extec, Enfield) mounted on a microtome (Isomet 1000, Buehler Ltd.) under water spray, at a calibrated speed of 250 rpm, and at a point 9 mm from the root apex, measured using a 0.01-mm calibrated digital caliper (IV Electronic Caliper, Fowler/Sylvac). After sectioning, five points were defined using a carbide bur #1/4, as a reference pattern to synchronize the measurements of specimens and CBCT scans, markings on the surface of each sample (X-axis - width, Y-axis - height, and Z-axis - depth). Samples were held stable using condensation silicone, and their axial surface was parallel to the ground. The posts were measured using a 0-25 mm/0.001 mm digital micrometer (Mitutoyo, Suzano, SP, Brazil) calibrated (certificate #07355/8) according to the relevant norms (ABNT NBR/ISO IEC 170/25 CAL #0031, PML 0003). The dimensions of the original posts were standard reference (control group) of comparison with the measurements obtained using the BAR filter on CBCT images. The micrometer was held stable on a leveled prefabricated platform, which was lifted to

Blooming artifact reduction with new CBCT software

C. Estrela et al.

the position for measurement using a metallic elevator. The active end of the digital micrometer, measuring 0.3 mm in diameter, was placed on the samples following the reference of the buccolingual and mesiodistal markings, using an operative microscope (25×, Alliance, São Carlos, SP, Brazil). A pilot study was conducted with one third of the sample to standardize measurements and reduce the possibility of negative events. Two observers with at least 15 years of experience each measured the samples at the same time. The level of interobserver agreement was assessed by kappa statistics.

Measurement of Specimens Using the e-Vol DX Software

Images were acquired using the DICOM format and a 13 bits PreXion 3D Elite CT scanner (PreXion Inc., San Mateo, CA, USA). Scanner parameters were: isotropic voxel size of 0.100 mm; FOV of 56 mm x 52 mm diameter by height; 37-s exposures and 512 exposures per capture; focal spot of 0.20 mm x 0.20 mm; X-ray output of 90 kVp; current of 4 mA; and total beam filtration of >2.5 mm of Al.

The DICOM file was processed using the e-Vol DX software (CDT Software, Bauru, SP, Brazil) on a desktop computer equipped with Windows 10 (Microsoft Corporation, Redmond, WA, USA), a 4.1-GHz i7-8750 processor (Intel Corporation, Santa Clara, CA, USA) and an 8-GB NVDIA GTX 1070 graphics card (NVIDIA Corporation). The captured images were visualized and analyzed using a 27-inch P2719H monitor with a resolution of 1920 x 1080 pixels at 60 Hz (DELL Inc., Eldorado do Sul, RS, Brazil).

For measurements, post diameters on the CBCT scans, the markings were synchronized on the samples according to X-, Y- and Z-axes and, when necessary, CBCT scans were repositioned to correct parallax errors. The e-Vol DX software was used to measure the diameter of the posts on the CBCT scans included in this study (13,17). The exact points to be measured, such as the marking on the edge of the anatomic structures, were defined, and the intermediate grade of the grayscale was adjusted on the CBCT scan. Thin, 0.10-mm slices were obtained from the 3D slices reconstructed using the filter for measurements, and the edge of the anatomic surface was defined on the axial plane. Positions in 3D mode were replicated in multiplanar CBCT image reconstruction, and the correct position was defined using a previously described positioning guide (17). After that, 3D density was adjusted to be on the same dimension as the 2D image. Therefore, dimension was calibrated so that 3D and 2D modes are coincident. This calibration was only performed at the beginning of measurements. From then on, the intermediate grade of the grayscale was checked on the CBCT scans. After one

side was done, the guide was moved to the other side, and the same guidelines were followed. The position of the markings was defined on the other edge using the 2D mode as reference.

The sample was positioned and first the color map tool was used. This tool displayed grayscale images in different colors, in the same way as the signal intensity of the material that composed teeth and posts, as interpreted by the software. White or hyperdense images of intracanal posts were primarily displayed in red. All images that were initially red were successively tested using the BAR filter, and blooming was checked using the four different filter intensities, BAR 1, 2, 3 and 4, as well as their different adjustments of brightness, contrast, improvement and dynamic range. The final check was performed on the grayscale image, which visually confirmed the outline of the object without any invasion of the hyperdense image into neighboring structures. Filters were selected according to the image color reformatting, and the peripheral area of the post under evaluation was in a color other than red.

The filters selected for the analysis of the samples were: BAR 1 for the gold alloy posts; BAR 2 for the low-fusion alloy posts; and BAR 3 for the anatomically customized glass fiber posts. The levels of brightness, contrast and improvement were automatically predetermined by the software. The linear measurement tool was set to "millimeter", and the mesiodistal (MD) and buccolingual (BL) diameters were traced and measured on the scans following the markings on the samples. The material of the anatomically customized glass fiber posts was less dense and not affected by secondary irradiation. Therefore, the limits of the edge of the post were identified on the CBCT scans, and only one measurement was performed. Beam hardening and scattering are inherent to CT acquisition and affect image outlines. Therefore, MD measurements (X-axis) were made using the most external point of the outline of the post image, that is, the external blooming area, and the internal point of the blooming artifact, which corresponded to the hyperdense margin of the post image. The same procedure was used for the BL measurement (Y-axis) (Fig. 1).

The mean value of the two measurements was calculated. The measures of metal posts and anatomically customized glass fiber posts were recorded on an Excel spreadsheet for statistical analysis (Table 1). The analysis of CBCT scans were conducted by two observers (specialist in dental radiology, previously trained to use this software and with more than 15 years of experience). The level of interobserver agreement was evaluated by kappa statistics.

Statistical Analysis

Statistical model residuals showed heteroscedasticity

and significant differences from normal distribution. Therefore, the Van der Waerden nonparametric analysis of variance was used, followed by the Tukey test applied to normalized data. The level of significance was set at $\alpha = 5\%$.

Results

There were no significant differences ($p > 0.05$) in diameters of intracanal posts measured in MD and BL directions using the micrometer (control group) or the CBCT scans after the application of the e-Vol DX BAR filter (Table 1, Fig. 2). The Kappa value for interobserver agreement considering the measurement of posts with micrometer and CBCT scans using e-Vol DX software ranged from 0.89-0.96.

Discussion

Blooming artifacts were not identified in any sample with metallic post, and there was no effect altering the image on adjacent root structures. These data showed that the e-Vol DX CBCT software did not induce dimensional volumetric expansion avoiding blooming artifacts.

The definition of a consolidated endodontic treatment protocol depends on diagnostic accuracy, adequate planning and appropriate clinical decision-making (13,18,19). However, the inappropriate interpretation of imaging findings may induce confusion and diagnostic errors, as well as subsequent incorrect planning and misguided decision making (7). Artifacts resulting from solid or metallic structures made of high-density materials distort object shape and contrast. Successive advances in the knowledge of artifact production on CBCT scans (6,8-11,20-24) have enabled the detection of dimensional changes and artifacts on CBCT scans of dental materials and intracanal posts. They have also elucidated their effects on the diagnosis of perforations and root fractures and motivated studies to improve the understanding of these challenging conditions, so that errors in decision-making may be reduced. The effect of intracanal gold alloy, silver alloy, glass fiber, carbon fiber and prefabricated metal posts on the dimensions on CBCT scans of endodontically treated teeth showed a variation of 7.7% to 100% of the corresponding real dimensions. Gold alloy and silver alloy posts showed greater variations than glass fiber, carbon fiber and prefabricated metal posts (9). Root canals sealers, with or without gutta-percha cones, showed volume
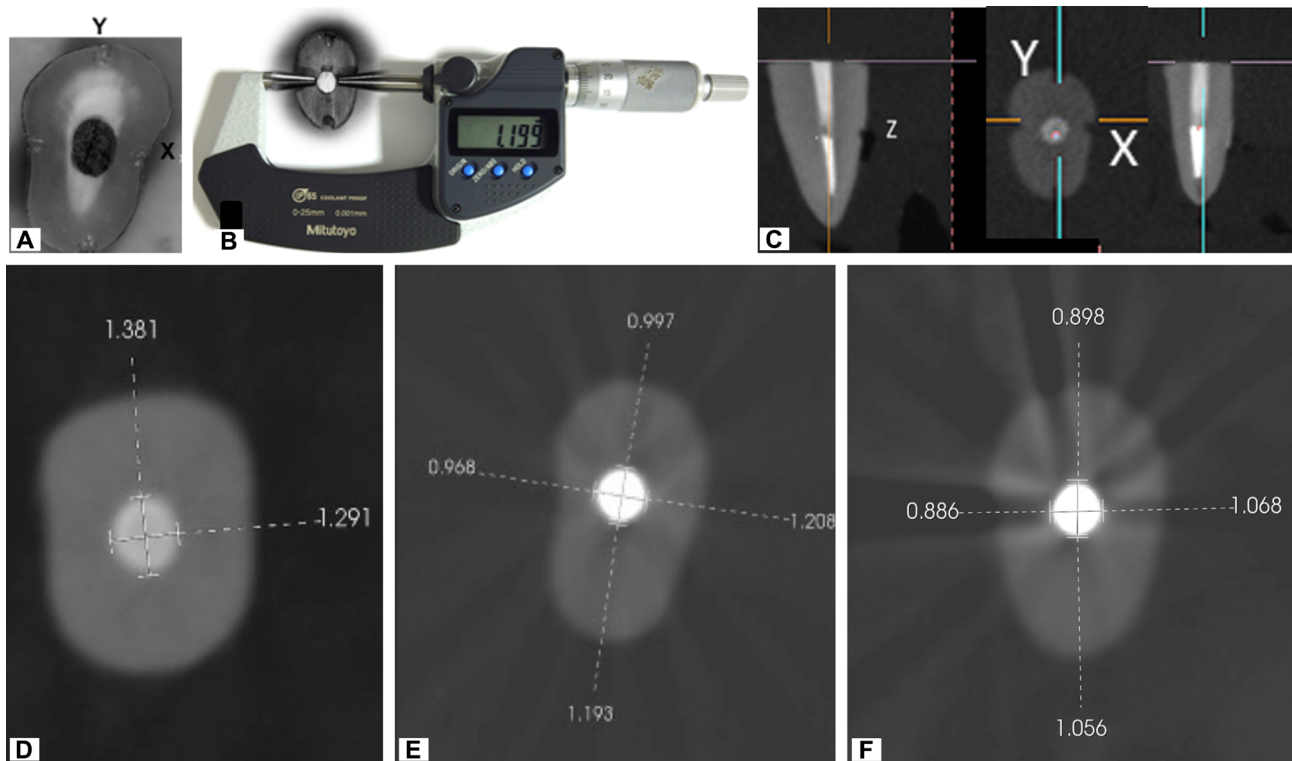
Figure 1. (A) Illustration of markings on the X-, Y- and Z-axes on the sample surface; (B) digital micrometer, each sample was first separated from the others using the crop tool and then aligned to the three anatomical planes - axial, coronal and sagittal - so that the sliced surface was parallel to the ground. To measure post diameters on the CBCT scans, the markings were synchronized on the samples according to X-, Y- and Z-axes; (D) Section/axial plane image of the anatomical fiberglass post sample using BAR 3 filter; (E) Image/axial plane image of the low fusion alloy post sample using BAR 2 filter; (F) Axial section/axial plane image of gold alloy metal post sample using BAR 1 filter. MD measurements (X-axis) were made using the most external point of the outline of the post image, that is, the external blooming area, and the internal point of the blooming artifact, which corresponded to the hyperdense margin of the post image. The same procedure was used for the BL measurement (Y-axis).

discrepancies on CBCT scans, with values 9% to 100% greater than the dimensions of the original specimens (10).

In the present study, some steps had to be taken to ensure that the measurements of intracanal posts were accurate and that specimen positioning was the same on CBCT scans: standardization of root and post length; specimen mounting and held stable on micrometer; manufacture and stability of an elevating platform for the uniform use of the micrometer; placement of markings for three guiding points (X-axis - width; Y-axis - height; Z-axis - depth) on the original specimens for the subsequent synchronization and measurement of the same points on CBCT scans of the intracanal posts. Adjustments were made for parallax correction when necessary. A specific tool, used as a positioning guide and for the definition of edges and limits for measurements, was developed for micrometric measurements and applied using the e-Vol DX software, together with synchronization for color map analysis (17).
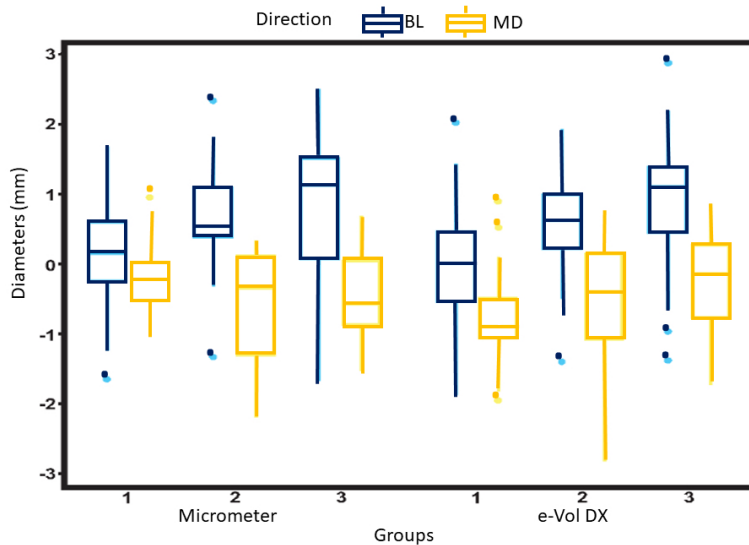
Figure 2. Values of MD and BL diameters of anatomically customized glass fiber posts (1), low-fusion alloy posts (2) and gold alloy posts (3) using a micrometer and CBCT scans after application of e-Vol DX BAR filter.

C. Estrela et al.

Table 1. Buccolingual (BL) and mesiodistal (MD) post diameters (mm) measured using a micrometer and CBCT scans obtained using the e-Vol DX software

Sample	Anatomical fiberglass				Low fusion alloy				Gold alloy			
	Micrometer		e-Vol DX		Micrometer		e-Vol DX		Micrometer		e-Vol DX	
	B-P	M-D	B-P	M-D	B-P	M-D	B-P	M-D	B-P	M-D	B-P	M-D
1	1.331	1.248	1.318	1.285	1.375	1.274	1.334	1.302	1.649	1.281	1.514	1.249
2	1.994	1.139	1.941	1.137	1.374	1.071	1.457	1.140	2.026	1.244	1.946	1.284
3	1.256	1.181	1.201	1.110	2.224	1.281	2.141	1.352	1.431	1.267	1.384	1.409
4	1.066	1.137	1.062	1.161	1.291	1.103	1.200	1.017	1.065	1.162	1.087	1.152
5	1.537	1.386	1.503	1.231	1.277	1.173	1.274	1.204	1.746	1.214	1.776	1.049
6	1.247	1.290	1.132	1.079	2.063	1.303	1.998	1.277	1.932	1.308	1.835	1.338
7	1.172	1.225	1.149	1.149	1.380	1.013	1.211	0,971	1.978	1.373	1.972	1.473
8	1.426	1.270	1.332	1.132	1.573	1.233	1.442	1.220	1.184	1.181	1.133	1.123
9	1.202	1.191	1.156	1.178	1.474	1.323	1.540	1.435	1.893	1.101	1.708	1.074
10	1.426	1.453	1.384	1.122	1.753	1.235	1.675	1.278	1.912	1.207	1.912	1.294
11	1.562	1.438	1.480	1.408	1.399	1.321	1.363	1.315	2.165	1.138	2.170	1.317
12	1.250	1.206	1.240	1.155	1.409	1.359	1.432	1.409	1.519	1.362	1.484	1.537
13	1.275	1.238	1.277	1.200	1.677	1.311	1.626	1.505	1.145	1.181	1.169	1.229
14	1.233	1.207	1.187	1.094	1.088	1.093	1.082	1.126	1.286	1.146	1.386	1.243
15	1.781	1.583	1.659	1.544	1.835	1.071	1.670	0,936	2.088	1.470	2.050	1.080
16	2.012	1.138	2.148	1.118	1.565	1.215	1.530	1.229	1.202	1.164	1.197	1.236
17	1.096	1.115	1.038	1.045	1.869	0,997	1.656	0,950	1.776	1.109	1.857	1.324
18	1.299	1.231	1.289	1.137	1.274	1.182	1.339	1.200	1.171	1.072	1.238	1.108
19	1.432	1.261	1.385	1.292	1.448	1.294	1.339	1.206	1.595	1.134	1.507	1.159
20	1.202	1.112	1.193	1.030	1.371	1.082	1.317	1.115	1.957	1.113	1.899	1.263
21	1.308	1.229	1.265	1.134	1.222	1.158	1.254	1.087	2.300	1.334	2.331	1.393

The e-Vol DX CBCT software present one of the features associated with the compatibility with all current CBCT scanners, and the capacity to export DICOM Data, a more comprehensive brightness and contrast, the custom slice thickness adjustment, the custom sharpening adjustment, the advanced noise reduction algorithm that enhances image quality. The image capture reaches 192-dpi screen resolution and option of 384 resolution, in contrast with the 96-dpi screen resolution of similar packages (13).

Several alternatives for metal artifact correction during CBCT image acquisition, reconstruction or other procedures have been tested (14-16,21,24-33). A metal artifact reduction (MAR) algorithm has been evaluated (28) using CBCT scans of dental materials, such as dental amalgam and copper-aluminum alloy. The scans were obtained at different FOV and voxel sizes. Results revealed that algorithm efficacy in reducing metal artifacts was similar for the different FOV and voxel parameters under study. Imaging protocols and the use of the MAR algorithm should be based on selection criteria, which should be individualized for each case (28). The quality of CBCT scans was verified using free software, which has low cost and required little time to operate (16). A macro program was developed using the ImageJ software (U. S. National Institutes of Health, Bethesda, MA, USA) to evaluate the quality parameters of images obtained using three different CBCT scanners. Eight parameters were selected: uniformity, sign-to-noise ratio, contrast-to-noise ratio, spatial resolution, artifact index, geometric accuracy and low-contrast resolution. No significant differences in presence of artifacts were found in the comparison of protocols. The influence of the metal artifact reduction (MAR) tool using two scanners, in the diagnosis of fractured instruments in root canals of mandibular molars with or without canal fillings, was determined recently (34). The MAR tool did not increase the detection of fractured endodontic instruments or reduce image noise. Therefore, the MAR tool was not recommended for evaluations of fractured endodontic instruments in mandibular molars with or without root fillings (34). Pauwels et al. (35) discussed important principles of image acquisition and reconstruction. For reconstruction, CBCT scans may be manipulated in different ways to improve visualization of anatomic structures and lesions. The most basic manipulation improves image contrast, and only part of the full gray value range is displayed. The full contrast of the display monitor, as well as the human eye, is applied to this specific gray value range. These operations may have different purposes: in CBCT, they are primarily used to improve contrast in the bone density range, which corresponds to bone gray values (35).

Bueno et al. (13) reported that the principle of image capture using a photo camera is crucial to understand and use the e-Vol DX software, because image capture essentially defines final quality (13). The RAW image format (native digital camera file) captures all data recorded by the sensor, from a large number of sensor pixels. Some filters were developed for this software, such as BAR (blooming artifact reduction), have been adjusted to the principles of the RAW format, which preserved image quality and may potentially recover under- or overexposed areas. These filters prevent the loss of image quality and improve saturation and brightness of specific areas, as the light areas of the image take up a substantial amount of space in the file. They also prevent the loss of image quality by using both blown highlight and gray, which usually turns into white. Technical and scientific knowledge about digital photography, and the fact that the free area of an image takes up almost half of the space in the file, are signs that the reduction of light or white area may result in substantial artifact reduction (13).

The clinical impact of artifact removal, described in this study of CBCT scans of endodontically treated teeth with metal posts that showed no dimensional changes or white contrast artifacts, lies in its accuracy of planning and diagnosis and, especially, in the fact that it ensures greater predictability when making clinical decisions. Considering the reason of being a pioneering study from the development and application of new software, further studies should compare the e-Vol DX software and other software packages used with different scanners.

The use of the BAR filter of the e-Vol DX CBCT software did not induce any dimensional changes on CBCT scans of low-fusion alloy, gold alloy and anatomically customized prefabricated intracanal posts, which was confirmed by comparing the results with measurements made using a micrometer on original posts. The use of the BAR filter eliminated blooming artifacts.

Resumo

Este estudo avaliou as dimensões de pinos intrarradiculares usando um novo software de tomografia computadorizada de feixe cônico (TCFC) e um micrômetro digital, e verificou o potencial da redução do artefato de contraste do branco. Sessenta e três dentes humanos unirradiculares foram modelados, obturados, preparados para colocação de pinos e distribuídos em três grupos: G1: pino de fibra de vidro pré-fabricado anatômico; G2: pino metálico de liga de baixa fusão; G3: pino metálico de liga de ouro. Após a confecção e cimentação dos pinos com RelyX U200®, os espécimes foram cortados no sentido axial a 9 mm do ápice radicular, sendo efetuadas marcações em suas superfícies radiculares (eixos X, Y e Z) para orientação das medidas e sincronizações das imagens. Foi utilizado um micrômetro digital para a mensuração das dimensões dos pinos originais (grupo controle) associado ao microscópio operatório. Posteriormente, as imagens em TCFC foram obtidas usando o PreXion 3D Elite®. Para a mensuração dos pinos nas imagens de TCFC utilizou-se o arquivo DICOM e a ferramenta de medida do software e-Vol DX, configurada para medidas milesimais, com o filtro BAR (Blooming Artifact Reduction). Os dados estatísticos foram avaliados com a análise de variância não-paramétrica de Van der Waerden, seguida pelo Teste de Tukey aplicado aos dados normalizados.

O nível de significância foi de α = 5%. Os resultados mostraram que as medidas dos diâmetros dos pinos intrarradiculares (fibra de vidro anatômico, metálico liga de baixa fusão, e em liga de ouro) usando o software e-Vol DX e o micrômetro não mostram diferenças significativas entre si. O uso do filtro BAR do software e-Vol DX não induziu diferenças dimensionais nas imagens de TCFC dos pinos quando comparadas às medidas realizadas com o micrômetro sobre os pinos originais. O uso do filtro BAR eliminou artefatos de contraste do branco.

Acknowledgements

References

1. Arai Y, Tammisalo E, Iwai K, Hashimoto K, Shinoda K. Development of a compact computed tomographic apparatus for dental use. Dentomaxillofac Radiol 1999;28:245-248.

2. Hargreaves KM, Diogenes A, Teixeira FB. Treatment options: biological basis of regenerative endodontic procedures. J Endod 2013;39:S30-S43.

3. Scarfe WC, Farman AG, Sukovic P. Clinical applications of cone-beam computed tomography in dental practice. J Can Dent Ass 2007;72:75-80.

4. Estrela C, Bueno MR, Leles CR, Azevedo BC, Azevedo JR. Accuracy of cone beam computed tomography and panoramic and periapical radiography for detection of apical periodontitis. J Endod 2008;34:273-279.

5. Mota de Almeida FJ, Knutsson K, Flygare L. The effect of cone beam CT (CBCT) on therapeutic decision-making in endodontics. Dentomaxillofac Radiol 2014;43:20130137.

6. Barrett JF, Keat N. Artifacts in CT: recognition and avoidance. Radiographics 2004;24:1679-1691.

7. Bueno MR, Estrela C, Figueiredo JAP, Azevedo BC. Map-reading strategy to diagnose root perforations near metallic intracanal posts by using cone beam computed tomography. J Endod 2011;37:85-90.

8. Anbu R, Nandini S, Velmurugan N. Volumetric analysis of root fillings using spiral computed tomography: an in vitro study. Int Endod J 2010;43:64-68.

9. Estrela C, Bueno MR, Silva JA, Porto OCL, Leles CR, Azevedo BC. Effect of intracanal posts on dimensions of cone beam computed tomography images of endodontically treated teeth. Dent Press Endod 2011;1:28-36.

10. Decurcio DA, Bueno MR, Alencar AH, Porto OCL, Azevedo BC, Estrela C. Effect of root canal filling materials on dimensions of cone-beam computed tomography images. J Appl Oral Sci 2012;20:260-267.

11. Vasconcelos KF, Nicolielo LF, Nascimento MC, Haiter-Neto F, Bóscolo FN, et al. Artefact expression. associated with several cone-beam computed tomographic machines when imaging root filled teeth. Int Endod J 2015;48:994-1000.

12. Huybrechts B, Bud M, Bergmans L, Lambrechts P, Jacobs R. Void detection in root fillings using intraoral analogue, intraoral digital and cone beam CT images. Int Endod J 2009;42:675-685.

13. Bueno MR, Estrela C, Azevedo BC, Diogenes A. Development of a new cone-beam computed tomography software for endodontic diagnosis. Braz Dent J 2018;29:517-529.

14. Neves FS, Freitas DQ, Campos PSF, Ekestubbe A, Lofthag-Hansen S. Evaluation of cone-beam computed tomography in the diagnosis of vertical root fractures: the influence of imaging modes and root canal materials. J Endod 2014;40:1530-1536.

15. Kocasarac HD, Yigit DH, Bechara B, Sinanoglu A, Noujeim M. Contrast-to-noise ratio with different settings in a CBCT machine in presence of different root-end filling materials: an in vitro study. Dentomaxillofac Radiol 2016;45:20160012.

16. Oliveira MVL, Santos AC, Paulo G, Campos PSF, Santos J. Application of a newly developed software program for image quality assessment in cone beam computed tomography. Imag Sci Dent 2017;47:75-86.

17. Bueno MR, Estrela CRA, Granjeiro JM, Sousa-Neto MD, Estrela C. Method to determine the root canal anatomic dimension by using a new cone-beam computed tomography software. Braz Dent J 2019;30:3-11.

18. Estrela C, Holland R, Estrela CR, Alencar AHG, Sousa-Neto MD, Pecora JD. Characterization of successful root canal treatment. Braz Dent J 2014;25:3-11.

19. Estrela C, Couto GS, Bueno MR, Bueno KG, Estrela LRA, Porto OCL, et al. Apical foramen position in relation to proximal root surfaces of human permanent teeth determined by using a new cone-beam computed tomographic software. J Endod 2018;44:1741-1748.

20. Katsumata A, Hirukawa A, Noujeim M, Okumura S, Naitoh M, Masami M, Ariji E, Langlais RP. Image artifact in dental cone-beam CT. Oral Sur Oral Med Oral Pathol Oral Radiol Endod 2006;101:652-657.

21. Schulze R, Heil U, Gross D, Bruellmann DD, Dranischnikow E, Schwanecke U, Schoemer E. Artefacts in CBCT: a review. Dentomaxillofac Radiol 2011;40: 265-273.

22. Bechara BB, McMahan AC, Moore WS, Noujeim M, Geha H, Teixeira FB. Contrast-to-noise ratio difference in small field of view cone beam computed tomography machines. J Oral Sci 2012;54:227-232.

23. Bechara BB, Moore WS, McMahan CA, Noujeim M. Metal artifact reduction with cone beam CT: An in vitro study. Dentomaxillofac Radiol 2012;41:248-253.

24. Bechara B, McMahan CA, Moore WS, Noujeim M, Teixeira FB, Geha H. Cone beam CT scans with and without artefact reduction in root fracture detection of endodontically treated teeth. Dentomaxillofac Radiol 2013;42:20120245.

25. Likubo M, Osano T, Sano T, Katsumata A, Ariji E, Kobayashi K, Sasano T, Wakoh M, Seki K, Kojima I, et al. Root canal filling materials spread pattern mimicking root fractures in dental CBCT images. Oral Sur Oral Med Oral Pathol Oral Radiol Endod 2015;120:521-527.

26. Barbosa GLR, Sousa-Melo SL, Alencar PNB, Nascimento MC, Almeida SM. Performance of an artefact reduction algorithm in the diagnosis of in vitro vertical root fracture in four different root filling conditions on CBCT images. Int Endod J 2016;49:500-506.

27. Celikten B, Jacobs R, Vasconcelos KF, Huang Y, Nicolielo LFP, Orhan K. Assessment of volumetric distortion artifact in filled root canals using different cone beam computed tomographic devices. J Endod 2017;43:1517-1521.

28. Queiroz PM, Gropp FC, Oliveira ML, Haiter-Neto F, Freitas DQ. Evaluation of the efficacy of a metal artifact reduction algorithm in different cone beam computed tomography scanning parameters. Oral Surg Oral Med Oral Pathol Oral Radiol Endod 2017;123:729-734.

29. Silva DM, Campos CN, Carvalho ACP, Devito KL. Diagnosis of mesiodistal vertical root fractures in teeth with metal posts: influence of applying filters in cone-beam computed tomography images at different resolutions. J Endod 2018;44:470-474.

30. Koç C, Kamburoglu K, Sönmez G, Yılmaz F, Gülen O, Karahan S. Ability to detect endodontic complications using three different cone beam computed tomography units with and without artefact reduction modes: an ex vivo study. Int Endod J 2019;52:725-736.

31. Fox A, Basrani B, Kishen A, Lam EWN. A novel method for characterizing beam hardening artifacts in cone-beam computed tomographic images. J Endod 2018;44:869-874.

32. Gambarini G, Ropini P, Piasecki L, R Costantini R, E Carneiro E, L Testarelli L, Dummer PMH. A preliminar assessment of a new dedicated endodontic software for use with CBCT images to evaluate the canal complexity of mandibular molars. Int Endod J 2018;51:259-268.

33. Freitas DQ, Nascimento EHL, Vasconcelos TV, Noujeim M. Diagnosis of external root resorption in teeth close and distant to zirconium implants: influence of acquisition parameters and artefacts produced during cone beam computed tomography. Int Endod J 2019;52:866-873.

34. Costa ED, Brasil DM, Queiroz PM, Verner FS, Junqueira RB, Freitas DQ. Use of the metal artefact reduction tool in the identification of fractured endodontic instruments in cone-beam computed tomography. Int Endod J 2020;53:506-512.

35. Pauwels R, Araki K, Siewerdsen JH, Thongvigitmanee SS. Technical aspects of dental CBCT: state of the art. Dentomaxillofac Radiol 2015;44:20140224.

C. Estrela et al.